

## Water-based condensation particle counters comparison near a major freeway with significant heavy-duty diesel traffic

Eon S. Lee<sup>a</sup>, Andrea Polidori<sup>b</sup>, Michael Koch<sup>b</sup>, Philip M. Fine<sup>b</sup>, Ahmed Mehadi<sup>c</sup>, Donald Hammond<sup>c</sup>, Jeffery N. Wright<sup>c</sup>, Antonio. H. Miguel<sup>c</sup>, Alberto Ayala<sup>c</sup>, Yifang Zhu<sup>a,\*</sup>

<sup>a</sup> University of California Los Angeles, Los Angeles, CA 90095, USA

<sup>b</sup> South Coast Air Quality Management District, Diamond Bar, CA 91765, USA

<sup>c</sup> California Environmental Protection Agency – Air Resources Board, Monitoring and Laboratory Division, P.O. Box 2815, Sacramento, CA 95812, USA

### H I G H L I G H T S

- ▶ Three TSI WCPC models (9 units) were compared for one month near a major freeway.
- ▶ The 3 models' responses were significantly different under downwind conditions.
- ▶ All units showed somewhat size dependency especially for smaller ultrafine particles.
- ▶ TSI model 3783 provides relatively consistent data among studied models.

### A R T I C L E I N F O

#### Article history:

Received 20 April 2012

Received in revised form

28 November 2012

Accepted 3 December 2012

#### Keywords:

WCPC

Ultrafine particles

Traffic emissions

Freeway

### A B S T R A C T

This study compares the instrumental performance of three TSI water-based condensation particle counter (WCPC) models measuring particle number concentrations in close proximity (15 m) to a major freeway that has a significant level of heavy-duty diesel traffic. The study focuses on examining instrument biases and performance differences by different WCPC models under realistic field operational conditions. Three TSI models (3781, 3783, and 3785) were operated for one month in triplicate (nine units in total) in parallel with two sets of Scanning Mobility Particle Sizer (SMPS) spectrometers for the concurrent measurement of particle size distributions. Inter-model bias under different wind directions were first evaluated using 1-min raw data. Although all three WCPC models agreed well in upwind conditions (lower particle number concentrations, in the range of  $10^3$ – $10^4$  particles  $\text{cm}^{-3}$ ), the three models' responses were significantly different under downwind conditions (higher particle number concentrations, above  $10^4$  particles  $\text{cm}^{-3}$ ). In an effort to increase inter-model linear correlations, we evaluated the results of using longer averaging time intervals. An averaging time of at least 15 min was found to achieve  $R^2$  values of 0.96 or higher when comparing all three models. Similar results were observed for intra-model comparisons for each of the three models. This strong linear relationship helped identify instrument bias related to particle number concentrations and particle size distributions. The TSI 3783 produced the highest particle counts, followed by TSI 3785, which reported 11% lower during downwind conditions than TSI 3783. TSI 3781 recorded particle number concentrations that were 24% lower than those observed by TSI 3783 during downwind condition. We found that TSI 3781 underestimated particles with a count median diameter less than 45 nm. Although the particle size dependency of instrument performance was found the most significant in TSI 3781, both models 3783 and 3785 showed somewhat size dependency. In addition, within each tested WCPC model, one unit was found to count significantly different and be more sensitive to particle size than the other two. Finally, exponential regression analysis was used to numerically quantify instrumental inter-model bias. Correction equations are proposed to adjust the TSI 3781 and 3785 data to the most recent model TSI 3783.

© 2012 Elsevier Ltd. All rights reserved.

\* Corresponding author. Tel.: +1 310 825 4324; fax: +1 310 794 2106.

E-mail address: [Yifang@ucla.edu](mailto:Yifang@ucla.edu) (Y. Zhu).

## 1. Introduction

Ultrafine particles (UFPs,  $D_p < 100$  nm) are of a significant health concern. Their small size enables them to penetrate into the pulmonary system at a high deposition rate (Jaques and Kim, 2000), subsequently causing inflammatory responses and chronic cardiovascular diseases (Gilmour et al., 2004). Deleterious health effects from UFPs also include inter-organ translocation, which may potentially impose burdens in the liver, spleen, kidneys, and brain (Donaldson et al., 2002; Kreyling et al., 2002; Oberdorster et al., 2002). Although the degree of the reported particle deposition rates varies, scientists agree that the translocation and deleterious health effects of these particles are primarily due to their chemical composition, small size, high surface area, and high number concentrations.

However, the accurate and precise measurement of UFP number concentration is still a challenge. To overcome this challenge, a fundamental concept of condensation particle counting (CPC) technique was first introduced in the 19th century which then became widely adopted (Aitken, 1890; McMurry, 2000). The CPC approach takes advantage of the heterogeneous particle condensation which promotes the growth of sampled UFPs to micron-sized particles (i.e., a size that can be optically detected by a photodetector) under a controlled super-saturation condition. Therefore, the particle detection efficiency also relies on particle condensation processes in supersaturated working fluid (Stolzenburg and McMurry, 1991). As a result, particle counting efficiency is affected not only by design parameters (e.g., working fluid and temperature between saturator and growth tube) but also by different physico-chemical properties of sample particles (Iida et al., 2009; Kulmala et al., 2007; Petaja et al., 2006).

For a long time, butanol has been used as the working fluid for CPCs. In 2003, TSI introduced the first laminar flow water-based CPC (WCPC), TSI model 3785. Using the laminar flow water condensation methodology (Hering and Stolzenburg, 2005; Hering et al., 2005), this instrument introduced a  $1 \text{ L min}^{-1}$  sample flow into a wet-walled tube, the second portion of which is heated (TSI, 2003). This creates a region of super-saturation that grows small particles to supermicrometer sized droplets that are counted optically. At low concentrations, the grown particles are counted individually, with a correction for dead time. Above about  $3 \times 10^4 \text{ cm}^{-3}$ , the WCPC 3785 enters into a photometric mode whereby particle concentration is inferred from the total light scattering from the cloud of droplets within the sensing chamber.

The TSI 3781, introduced in 2005, is a compact unit that has an aerosol flow of  $0.12 \text{ L min}^{-1}$ , but is otherwise based on the same laminar flow and water condensation technology as TSI 3785, and uses the same operating temperatures. One noted difference is that the 3781 does not have a photometric mode; instead it only uses dead-time corrected single particle counting (TSI, 2005).

The TSI 3783, introduced in 2011, is the first of the next generation of WCPCs. The 3783 uses a new design for the condensation growth tube that improves instrument performance at high particle concentrations and provides consistent lower detectable particle size across all concentrations. The 3783 has the same aerosol flow but different operating temperature, and like the 3781, it does not have a photometric mode, but instead uses dead-time corrected single particle counting throughout its concentration range (TSI, 2011). None of the instruments tested have a sheathed flow.

There is little information available regarding the response differences among different WCPC models, especially in the near-freeway environment. The present study examines and compares the performance (bias, precision, effect of particle number concentration, and particle size) of three different WCPCs, namely

TSI models 3781, 3783, and 3785. A detailed investigation on the origin of the observed differences due to instrument design factors is beyond the scope of the current work. A total of nine WCPC units comprising three units of each model were concurrently operated near a major freeway for one month. The most recent TSI model (i.e., TSI 3783) has been promoted as best suited for long-term field operation in both rural and heavily polluted environments (TSI, 2011). An accurate assessment of the performance of this up-to-date model can provide valuable information to assist air monitoring organizations with planning future UFP measurement studies. This intensive WCPC monitoring study was the beginning of an extended monitoring effort ( $\sim 6$  months) aimed at evaluating TSI 3783 for potential use in a regulatory-like monitoring network.

This paper focuses on intra-model precision and inter-model bias. Since there is no reference instrument for particle number concentrations, bias between instrument units is evaluated in lieu of accuracy. Using the high-resolution data acquired, we evaluated the effects of upwind (low particle concentrations,  $10^3$ – $10^4 \text{ particle cm}^{-3}$ ) and downwind (high particle concentrations, above  $10^4 \text{ particles cm}^{-3}$ ) conditions on WCPC instrument responses in a realistic near-freeway environment and further assessed the effects of particle number concentration and size distribution on intra-model precision and inter-model bias. We also investigated the effect of increasing averaging time intervals so as to increase inter-model correlation. Finally, 3-parameter exponential equations are proposed to provide correction factors to adjust for differences in response between older models (TSI 3781 and 3785) and the most recent model (TSI 3783). Findings regarding the performance and reliability of these three WCPCs and their ability to run unattended for long periods of time will be provided in a subsequent paper.

## 2. Methodology

### 2.1. Experimental

#### 2.1.1. Site description

Extensive field measurements were carried out to monitor UFPs near the 710 freeway in Long Beach, California, from May 16th to June 15th, 2011. An *in situ* monitoring trailer equipped with various particle instruments was operated in close proximity to the freeway (15 m from the eastern edge of the 710). The surrounding area was an open flat terrain without a significant source of UFPs other than the traffic emissions from the freeway. The immediate east side of the freeway includes a large flood plain area and the Los Angeles River. The sampling site was located 13 km north of the Long Beach harbor. Therefore, the freeway traffic was the primary source of UFPs at the sampling site. Fig. 1 illustrates the orientation of the freeway and the monitoring station. The 710 freeway generally runs from north to south but the studied section runs  $30^\circ$  to the east. The wind rose chart in Fig. 1 describes the presence of a distinct westerly wind, which is typical for this part of the South Coast Air Basin during this time of the year. In addition to this dominant westerly component, the study period was characterized by the typical afternoon onshore sea-breeze and weaker winds coming from all directions. For the purpose of this study, downwind conditions were defined when the wind direction was about perpendicular to the freeway center-line and at a  $300^\circ \pm 45^\circ$  angle. Similarly, upwind conditions referred to time periods when the wind direction was about perpendicular to the 710 center-line but at a  $120^\circ \pm 45^\circ$  angle. Upwind and downwind conditions accounted for 14% and 48% of all observed wind directions during the study period, respectively. The remaining 38% of the data were considered under other wind conditions in the analysis.

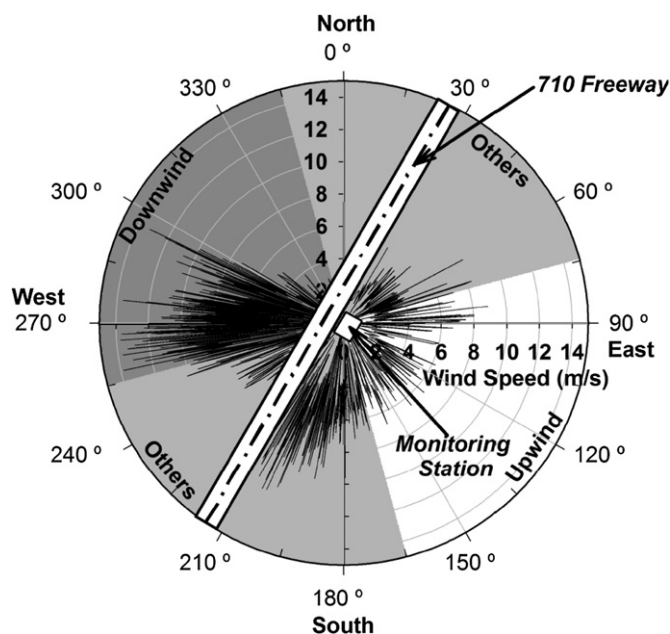


Fig. 1. A schematic of the sampling site including the orientation of the 710 freeway, the monitoring station, wind speed (radial) and wind direction (angular) data during the sampling period, and allocated upwind, downwind, and the other wind directions.

### 2.1.2. Traffic conditions

Traffic flow data near the sampling site were collected by means of two traffic sensors that are part of the CalTrans Performance Measurement System (PeMS): one for northbound traffic (PeMS ID 717966) and the other for southbound traffic (PeMS ID 717963) (CalTrans, 2010). These sensors were located approximately 600 m and 150 m from the monitoring station, respectively. Fig. 2 presents the overall diurnal traffic pattern changes for weekdays and weekends. The 710 freeway reached up to 1200 vehicles per 5 min around the morning and afternoon rush hours, whereas the minimum traffic volume was 150 vehicles per 5 min overnight. At this site, the 710 freeway traffic includes high heavy-duty diesel traffic flow that is approximately 18% of the total daily average.

### 2.1.3. Sampling and instrumentation

Meteorological parameters were measured by a weather station 10 m above the ground on top of the monitoring trailer. Temperature, humidity, wind direction, and wind speed were recorded at 1-min intervals. At the monitoring site, three units of each of the three WCPC models (3781, 3783, and 3785, TSI Inc., Shoreview, MN) were first synchronized and then set-up to concurrently record UFP concentrations at a 1-min sampling interval. Before doing data analysis, data were checked for alignment. Although all WCPCs have been synchronized, one- to two-minute differences among different units were found and manually corrected for better synchronization. To meet U.S. EPA particulate matter (PM) siting criteria while minimizing particle loss, an air intake manifold supplied the same ambient air sample, which was immediately distributed to each instrument through a series of conductive tubing of the same length (i.e., 1.5 m). All the particle instruments were calibrated by the manufacture prior to deployment and checked for flow and other parameters once every two weeks after deployment.

The manufacture published specifications of the three WCPC models are summarized in Table 1. The three models have a similar detectable particle size range with the same upper limit of 3  $\mu\text{m}$  and lower limits of 5, 6, and 7 nm for models 3785, 3781 and 3783, respectively. Even though maximum detectable particle count

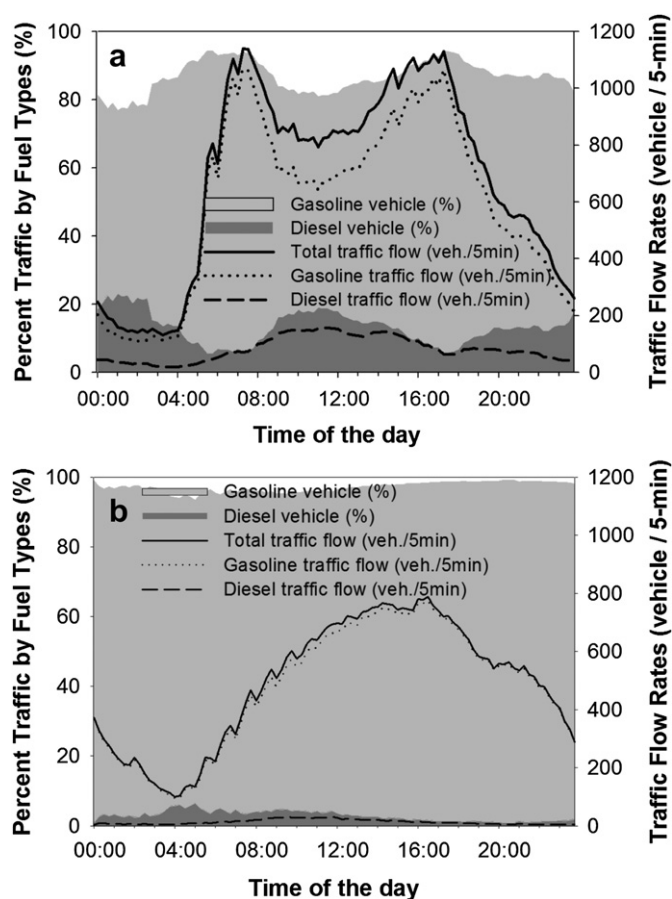


Fig. 2. Comparison of diurnal traffic pattern changes on freeway 710 during (a) weekdays and (b) weekends.

limits vary with different models, the highest particle number concentration measured during this study (approximately  $3 \times 10^5 \text{ cm}^{-3}$ ) was well below any of the highest detectable limits reported by the manufacturer for these three models (see Table 1). It was thus reasonable to expect that the three WCPC models should measure comparable values. However, it should be noted that inlet flow rates are different among the tested WCPCs (see Table 1) which may affect particle diffusion loss in the sampling line. For the average particle size distribution observed in the study, after considering different sampling flow rates, the disparities in diffusion losses to the sampling lines among the tested models were estimated to be less than 5% (i.e., 4.5% between models 3781 and 3783; 2.5% between models 3783 and 3785; and 2.0% between models 3781 and 3785) (Hinds, 1999). These diffusion loss differences were considered negligible and were not accounted for in the following inter- and intra-model comparisons.

Independent from the nine WCPC units, two sets of Scanning Mobility Particle Sizer (SMPS) spectrometers also continually monitored the UFP size distributions from the same sample air flow. The sample aerosols were first classified by particle size with Electrostatic Classifiers (TSI model 3080), and then by two additional WCPCs (TSI models 3785 and 3786) which quantified particle number concentration in each particle size bin. One SMPS was set to measure particles in the size range of 7.6–289 nm with a Long-DMA (TSI model 3081) while the other SMPS was set to measure 2.5–79.1 nm particles with a Nano-DMA (TSI model 3085). A 90-s sampling time and 30-s retrieval time were equally applied to achieve temporally comparable data from the two sets of SMPS systems. The SMPS data were used to better understand the effect

**Table 1**  
Specifications from manufacturer's instrument manuals of the three tested WCPC models (TSI 3781, 3783, and 3785).

Specifications	Model 3781	Model 3783	Model 3785
Year introduced	2005	2011	2003
Single particle counting with dead-time correction	All range	All range	Below $3 \times 10^4 \text{ cm}^{-3}$
Photometric mode	n/a	n/a	Above $3 \times 10^4 \text{ cm}^{-3}$
Detectable particle diameter ranges	6 nm–3 $\mu\text{m}$	7 nm–3 $\mu\text{m}$	5 nm–3 $\mu\text{m}$
Maximum detectable (# $\text{cm}^{-3}$ ) particle concentrations ( $\text{cm}^{-3}$ )	$5 \times 10^5$	$1 \times 10^6$	$1 \times 10^7$
Particle counting errors	$\pm 10\%$ at $5 \times 10^5 \text{ cm}^{-3}$	$\pm 10\%$ at $1 \times 10^6 \text{ cm}^{-3}$	$\pm 10\%$ at $2 \times 10^4 \text{ cm}^{-3}$
Aerosol flow rates ( $\text{L min}^{-1}$ )	$0.12 \pm 0.012$	$0.12 \pm 0.012$	$1.0 \pm 0.1$
Inlet flow rates ( $\text{L min}^{-1}$ )	$0.6 \pm 0.12$	$3 \pm 0.3$	1.035

of particle size on inter-model precision and intra-model bias as discussed in the result section.

## 2.2. Analytical

The data analysis focused on quantifying both intra-model precision and potential inter-model biases among three units of different models. The collected 1-min WCPC raw data were first classified with respect to upwind, downwind, and other conditions as illustrated in Fig. 1. The corresponding WCPC data were used to investigate instrument responses under different wind conditions. In an effort to improve inter- and intra-model correlation, we investigated the effect of using longer averaging time intervals (i.e., 5-min and 15-min) regardless of wind directions. It should be noted that only 15-min data resulting from averaging of 15 consecutive 1-min data observations were considered in our analysis. This accounts for more than 99% of the raw data used for analysis. Effects of particle number concentration range and particle count median diameter (CMD) on bias were then investigated. For inter-model

comparisons, the 15-min average concentrations from three units of the same model were utilized to represent each model. Biases related to the effect of particle concentration were studied for three particle number concentration ranges: low ( $10^3$ – $10^4 \text{ cm}^{-3}$ ), moderate ( $10^4$ – $10^5 \text{ cm}^{-3}$ ), and high ( $10^5$ – $3 \times 10^5 \text{ cm}^{-3}$ ). Using linear regressions, the coefficient of determination ( $R^2$ ) of each regression represented data variability in the corresponding concentration range. Furthermore, the investigation of the particle size distribution effects took into account the CMDs from each set of particle size distributions. The particle number concentration data were classified with respect to eight CMD ranges that were selected to include the same number of observations each. The Coefficients of Divergence (COD) was then used to estimate variances of WCPC data between any two compared WCPC models as follows:

$$\text{COD}_{jk} = \sqrt{\frac{1}{n} \sum_{i=1}^n \left( \frac{N_{ij} - N_{ik}}{N_{ij} + N_{ik}} \right)^2} \quad (1)$$

where,

$\text{COD}_{jk}$ : Coefficients of Divergence between two WCPC models (or units)  $j$  and  $k$

$n$ : Total number of observations

$i$ : Individual observation

$N$ : Particle number concentration ( $\text{cm}^{-3}$ )

The COD is a measure of homogeneity between two different WCPC data sets and ranges from 0 (homogeneous) to 1 (heterogeneous). In this study, the COD estimations were repeated for each

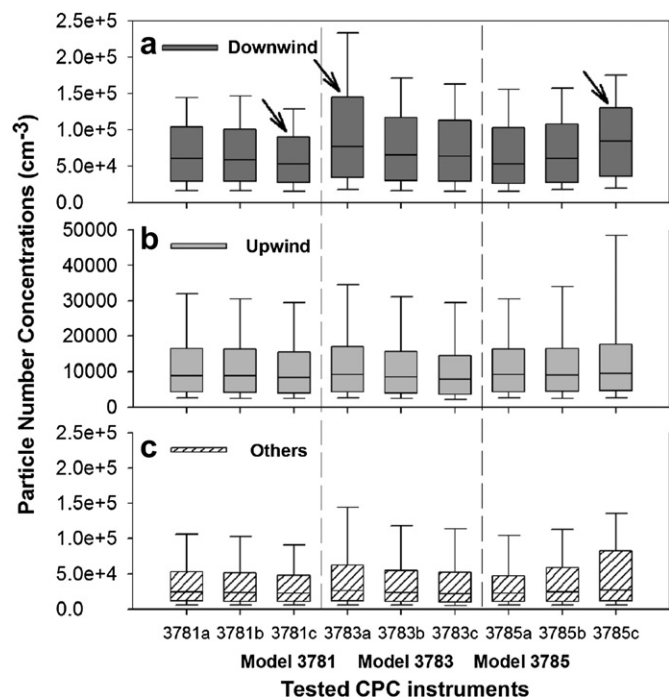


**Fig. 3.** Comparison among three tested WCPC TSI models (3781, 3783, and 3785) is provided 1-min averaged data for (a) downwind ( $300^\circ \pm 45^\circ$ ), (b) upwind ( $120^\circ \pm 45^\circ$ ), and (c) other wind conditions. Arrows indicate the unit that measured lower (i.e., 3781c) or higher (i.e., 3783a and 3785c) than the other two units of the same model based on visual observations. Under downwind conditions (a), TSI models 3781, 3783, and 3785 showed average concentrations of  $69,000 \text{ cm}^{-3}$ ,  $90,000 \text{ cm}^{-3}$ , and  $80,000 \text{ cm}^{-3}$ , respectively.

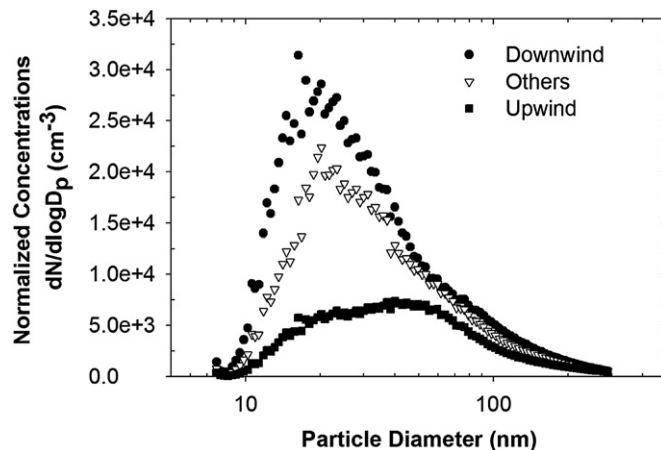


**Fig. 4.** Comparisons among particle size distributions measured and averaged under different wind directions (i.e., upwind, downwind, and others as depicted in Fig. 1) during the sampling period of one month.

CMD range and each model comparison. The estimated COD data are presented with the average values in each CMD range. Finally, we utilized a 3-parameter exponential regression analysis to numerically quantify potential instrument biases with respect to the observed particle number concentration ranges.

### 3. Results and discussions

#### 3.1. Inter- and intra-model comparisons under different wind conditions

Fig. 3 shows inter-model biases and intra-model precision using boxplots based on 1-min raw data under different wind directions.

Under upwind conditions, all nine units measured an average particle number concentration of approximately  $8000 \text{ cm}^{-3}$ . However, in downwind conditions one unit for each model provided measurements which, to some extent, were different from those recorded by the other two units of the same model. More specifically, the 3781c underestimated values compared with the other two units of model 3781; the 3783a and 3785c measured higher values than the other two units of the same model. This observation is further discussed in a later section (3.2.3. Effects of particle size distributions). Under other wind conditions (i.e., when the prevailing winds were mostly parallel to the freeway), average particle number concentrations were between the values observed in downwind and upwind conditions. Based on visual

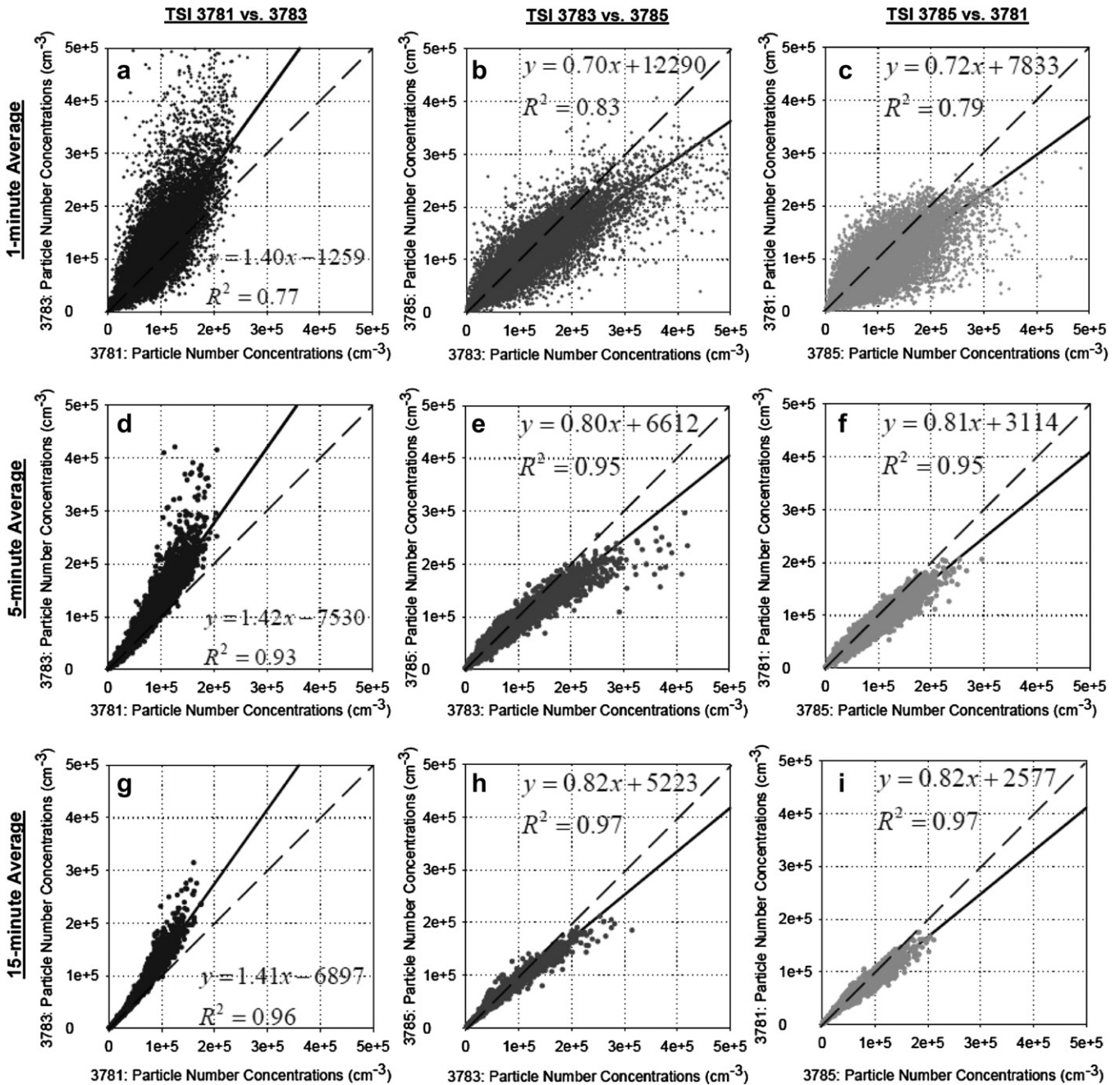


Fig. 5. Instrument response as a function of averaging time periods: 1-min (panels a–c), 5-min (panels d–f), and 15-min (panels g–i). For each panel, both x and y axis represent particle number concentrations in the range of  $0\text{--}5 \times 10^5 \text{ cm}^{-3}$ . With increasing averaging time periods (i.e., from top to bottom panels), the variability in the model performances is reduced.

observations, there did not appear to be any inter-model bias under these other wind conditions.

Under downwind conditions the average particle number concentration differed noticeably by different models. Specifically, models 3781, 3783, and 3785 showed average concentrations of  $69,000 \text{ cm}^{-3}$ ,  $90,000 \text{ cm}^{-3}$ , and  $80,000 \text{ cm}^{-3}$ , respectively (Fig. 3-a). The largest bias was observed for TSI 3781. It should be noted that the small bias between models 3783 and 3785 was present regardless of wind direction and, thus, for a wide range of particle concentrations. All three TSI 3781 units recorded approximately 26% and 12% lower particle number concentrations than models 3783 and 3785, respectively. The underestimations may have

resulted from TSI 3781's poor response to particles with CMD less than 45 nm as discussed in more details later.

To discover the underlying factors causing the observed inter-model biases (Fig. 3), average particle size distributions under upwind, downwind, and other wind conditions were determined (Fig. 4). While there was a predominant mode at 18 nm under downwind conditions, particle number concentrations were more evenly distributed throughout the measured size range under upwind conditions. Although particle size distribution measured under other wind conditions was similar to that under downwind conditions, the magnitude of particle concentration was lower and the size distribution curve lied between downwind and upwind

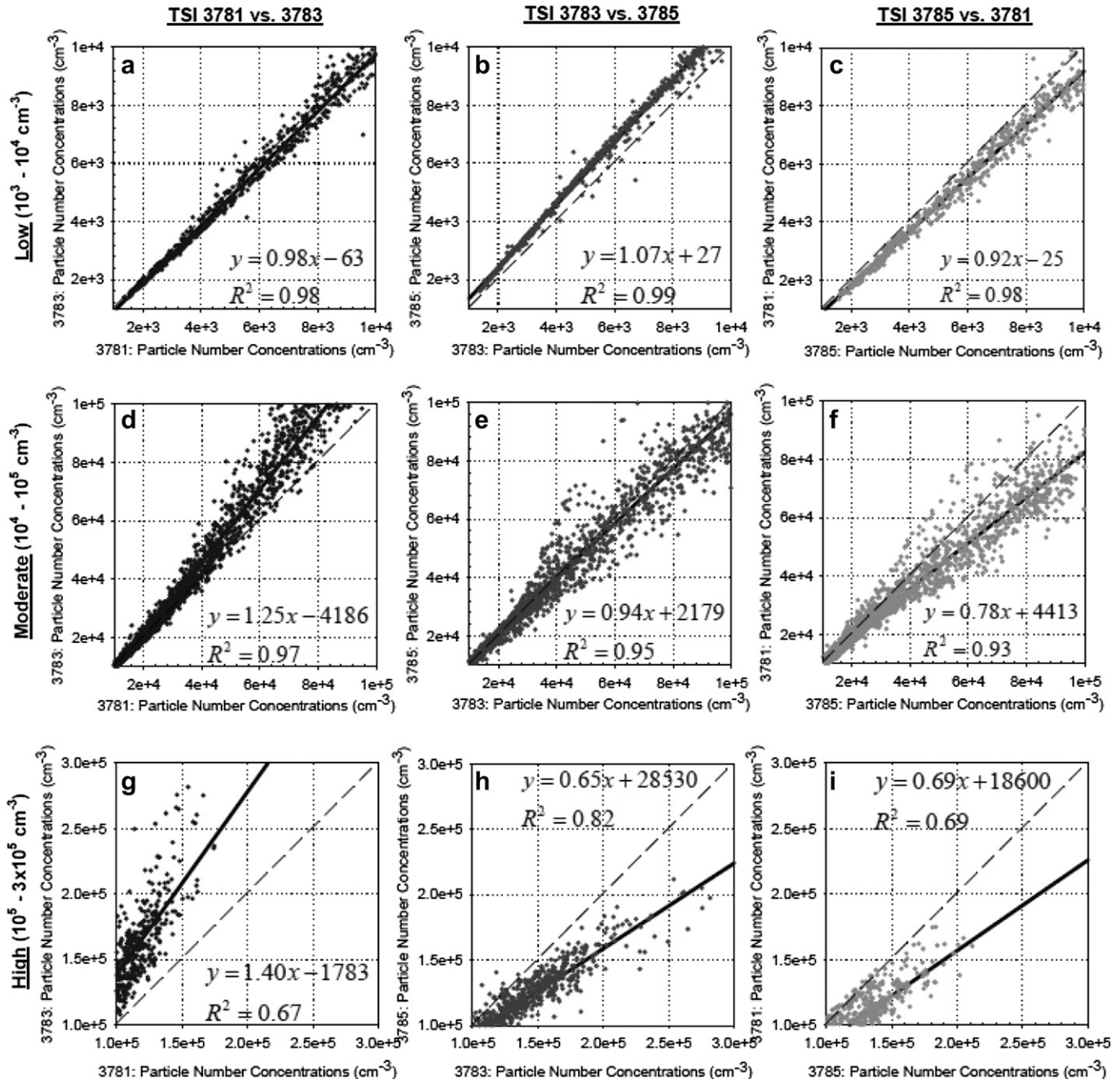


Fig. 6. Instrument response as a function of particle number concentration ranges: low (panels a–c,  $10^3$ – $10^4 \text{ cm}^{-3}$ ), moderate (panels d–f,  $10^4$ – $10^5 \text{ cm}^{-3}$ ), and high (panels g–i,  $10^5$ – $3 \times 10^5 \text{ cm}^{-3}$ ). With increasing source particle number concentrations (i.e., from top to bottom panels), the variability in the model performances also increases to a great extent (15-min averaged data provided).

**Table 2**

Summary of the linear regression results (i.e., slope ( $m$ ), intercept ( $i$ ), coefficient of determination ( $R^2$ ), and number of observations ( $n$ )) of intra-model comparisons by averaging time intervals and concentration ranges. Taking the 15-min averaging for example, we only included data when we had 15 out of the 15 1-min observations. This accounts for more than 99% of our available raw data.

Categories			TSI model 3781			TSI model 3783			TSI model 3785		
			a vs. b	b vs. c	c vs. a	a vs. b	b vs. c	c vs. a	a vs. b	b vs. c	c vs. a
Averaging time	1-min	$R^2$	<b>0.89</b>	<b>0.79</b>	<b>0.91</b>	<b>0.74</b>	<b>0.98</b>	<b>0.73</b>	<b>0.83</b>	<b>0.83</b>	<b>0.94</b>
		$M$	0.99	0.75	1.07	0.46	0.94	1.70	0.89	1.05	0.85
		$i$	-44	7018	2257	21,670	1075	-16,350	5239	9818	-2778
		$n$	41,848	41,848	41,848	41,847	41,847	41,847	41,848	41,848	41,848
	5-min	$R^2$	<b>0.98</b>	<b>0.93</b>	<b>0.96</b>	<b>0.89</b>	<b>0.99</b>	<b>0.88</b>	<b>0.98</b>	<b>0.97</b>	<b>0.98</b>
		$m$	1.02	0.83	1.09	0.58	0.95	1.59	0.97	1.17	0.83
		$i$	-1291	2987	1137	12,510	229	-10,770	887	3394	-1501
		$n$	8348	8348	8349	8370	8367	8370	7135	6901	6624
	15-min	$R^2$	<b>0.98</b>	<b>0.95</b>	<b>0.96</b>	<b>0.94</b>	<b>0.99</b>	<b>0.94</b>	<b>0.99</b>	<b>0.98</b>	<b>0.98</b>
		$m$	1.02	0.85	1.09	0.64	0.96	1.5	0.97	1.19	0.82
		$i$	-1110	2389	1018	8758	19	-8515	469	2257	-828
		$n$	2783	2783	2784	2790	2790	2790	2383	2303	2209
Concentration ranges (15-min)	Low	$R^2$	<b>0.97</b>	<b>0.96</b>	<b>0.99</b>	<b>0.99</b>	<b>0.99</b>	<b>0.99</b>	<b>0.99</b>	<b>0.97</b>	<b>0.98</b>
		$m$	0.95	0.95	1.06	0.91	0.93	1.17	0.96	1.09	0.91
		$i$	44	104	79	23	-1	6	54	17	121
		$n$	514	1851	418	537	1647	606	407	1263	334
	Moderate	$R^2$	<b>0.98</b>	<b>0.94</b>	<b>0.96</b>	<b>0.97</b>	<b>0.99</b>	<b>0.97</b>	<b>0.98</b>	<b>0.98</b>	<b>0.97</b>
		$m$	0.97	0.88	1.10	0.75	0.97	1.35	0.99	1.29	0.74
		$i$	403	1813	358	4352	-415	-3700	299	-568	2099
		$n$	514	1851	418	537	1647	606	439	1468	396
	High	$R^2$	<b>0.75</b>	<b>0.41</b>	<b>0.55</b>	<b>0.69</b>	<b>0.98</b>	<b>0.64</b>	<b>0.91</b>	<b>0.85</b>	<b>0.88</b>
		$m$	1.04	0.76	0.52	0.33	0.91	2.21	0.88	0.88	1.01
		$i$	-944	11,270	63,760	69,200	5530	-88,680	13,470	37,270	-22,540
		$n$	514	1846	417	537	1647	606	402	1388	347

conditions. This agrees well with previous work that documented the same tendency of upwind/downwind particle size distributions near the 710 freeway (Zhu et al., 2002). Thus, the particle number concentration and particle size might play important roles in explaining the observed discrepancies among different WPC models as discussed in the following sections.

### 3.2. Factors affecting inter- and intra-model precision and bias

#### 3.2.1. Effects of averaging time intervals

One approach to increase instrument comparability may be to increase the time-averaging period. Although all measurements aimed to achieve high-resolution (i.e., 1-min) data, interpretation of the data was challenging because of highly variable 1-min responses from the three WPC models. Increasing averaging time intervals increases instrument precision but information about short-term variability due to sudden increase or decrease in particle number concentration is lost. Although increased averaging-time could not distinctively present abrupt changes in concentration, it may be desirable to achieve appropriate instrument comparisons in a long-term sampling study. The collected 1-min raw data, regardless of wind directions, were then post-processed to produce data with an averaging time of 5 and 15 min(s). With 1-min data, the regression analyses found the lowest  $R^2$  of 0.77 for the comparison between models 3781 and 3783 (Fig. 5-a). Similarly, the  $R^2$  from the other two regressions with 1-min data remained at 0.83 and 0.79 in Fig. 5-b (3783 vs. 3785) and -c (3785 vs. 3781), respectively. The correlation between models 3783 and 3785 was stronger than the other comparisons with model 3781 (i.e., 3781 vs. 3783 and 3785 vs. 3781) for the 1-min data. Thus, it is possible that model 3781 was responsible for the low correlation results shown in Fig. 5-a and -c. The  $R^2$  values increased to 0.93 and higher with 5-min averaging time (Fig. 5-d through -f). With 15-min averaging time interval, all three inter-model comparisons clearly demonstrated correlation among the different models with an  $R^2$  0.96 or above (Fig. 5-g through -i). In the subsequent data analysis, only 15-min averaged data were used.

#### 3.2.2. Effects of particle number concentrations

Fig. 6 illustrates the effect of particle number concentration on the WPC responses for different models. A slope greater than 1 indicates a positive bias for the instrument along the y-axis, and a slope less than 1 indicates a positive bias for instrument on the x-axis. The intercept also needs to be considered. The confidence of the slope (bias) decreases as  $R^2$  decreases. In particular, inter-model correlations ( $R^2$ ) were consistently above 0.98 in the low particle concentration range ( $10^3$ – $10^4$   $\text{cm}^{-3}$ ; Fig. 6-a through -c). However, the  $R^2$  dropped when the particle number concentration ranged between  $10^4$  and  $10^5$   $\text{cm}^{-3}$  (Fig. 6-d through -f). Finally, all  $R^2$  values decreased further to 0.67 through 0.82 in the concentration range of  $10^5$ – $3 \times 10^5$   $\text{cm}^{-3}$  (Fig. 6-g through -i). Therefore, the variability

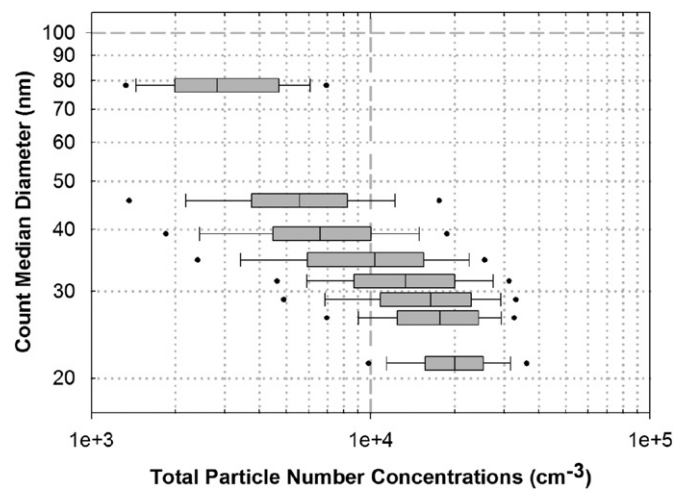


Fig. 7. Relationship between total particle number concentrations and corresponding particle count median diameters (CMD) from measured particle size distributions. The total particle number concentration increases as CMD decreases. Note that the same number of observations is allocated to each box using 15-min average data.

among these WCPC models increases as the particle concentration increases.

As the figures show, the magnitude of the measured concentrations varies by different instrument models and number concentration ranges. It should be noted that model 3781 repeatedly measured the lowest number concentrations for number concentrations above  $10^4 \text{ cm}^{-3}$ , followed by model 3785. Model 3783 showed higher number concentration readings than the other two models in general. This is not likely due to different detectable particle size ranges by the selected models. For example, Fig. 6 shows model 3783 measured the highest number concentrations in spite that it has a narrower detectable size range than that of the other two models. If detectable particle size ranges were the reason, model 3785 should have measured the highest number concentrations and the lowest number concentration should have been recorded by model 3783 as indicated by the instruments' specifications shown in Table 1. The bias between model 3783 and the other two models also increased as the concentration increased.

Although Fig. 6-h illustrates that model 3783 had the highest variability in particle concentration above  $10^5 \text{ cm}^{-3}$ , model 3783 responded similarly to model 3785 between  $10^4 \text{ cm}^{-3}$  and  $10^5 \text{ cm}^{-3}$  (Fig. 6-e), unlike the other two model comparisons in the same range (Fig. 6-d and -f). For particle concentration ranges below  $10^4 \text{ cm}^{-3}$ , the overall response of all three models were very similar. Another important observation is that model 3781 did not measure particle count up to the manufacturer-claimed instrument counting limit of  $5 \times 10^5 \text{ cm}^{-3}$ . As illustrated in Fig. 6-g and -i, model 3781 only measured up to  $2 \times 10^5 \text{ cm}^{-3}$  while the other two models measured particle number concentrations up to  $5 \times 10^5 \text{ cm}^{-3}$ . Although our dataset is limited, caution should probably be exercised when using model 3781 near combustion sources where relatively high particle number concentrations is expected.

In addition to inter-model comparisons, Table 2 summarizes linear regression results for correlations between instrument units of the same model, sorted by averaging time and concentration range. Using linear regression, individual instrument units were compared to another unit of the same model. There was strong intra-model variability among all three models indicating individual instrument may perform differently from another unit of the same model. In general, higher  $R^2$  values were observed with increasing averaging time intervals and at lower particle concentrations which corroborates findings in inter-model comparison as shown in Figs. 5 and 6. Conversely, the higher the concentration range, the lower the  $R^2$  values.

### 3.2.3. Effects of particle size distributions

Differences in inter-model responses were further studied with respect to CMD to assess the impacts of changes in particle size

distributions. Fig. 7 illustrates that the total particle number concentration increased when the CMD decreased, especially when the CMDs were between 20 and 30 nm. It should be noted that the same number of observations are presented in each box in Fig. 7. Thus, particle-counting instrument accuracy may be affected to a great extent by particles in this size range which constitute the majority of particles in term of number concentration near roadways.

The observed size-dependent counting efficiency helps to explain the considerable underestimations in particle count measurements for model 3781. Fig. 8 presents COD (Eq. (1)) changes across measured CMD ranges among different tested WCPC models when the particle concentrations are below  $1 \times 10^4 \text{ cm}^{-3}$  (Fig. 8-a) and above  $1 \times 10^4 \text{ cm}^{-3}$ . The COD becomes a measure of magnitude of divergence and the gradient of COD value indicates a series of changes in the magnitude of divergence. Fig. 8-a showed CODs were not only comparable (all remained less than 0.01) but also flat across CMDs when particle concentrations are below  $1 \times 10^4 \text{ cm}^{-3}$ . It suggests that there is hardly any particle size effect on instrument bias in this low particle concentration range. On the other hand, when particle concentrations are above  $1 \times 10^4 \text{ cm}^{-3}$  (Fig. 8-b), CODs started to diverge when CMDs are less than 45 nm. Models 3783 and 3785 demonstrated consistent performances with a low COD of approximately 0.005. Although there were differences in measurements between models 3783 and 3785 as discussed previously, the magnitude of these differences (i.e., COD) was minimal and consistent throughout all considered CMD ranges. In contrast, the COD between models 3781 and 3783 demonstrated greater divergence when CMDs were less than 45 nm. The divergence significantly increased as the particle CMD decreased. Thereby, the high COD gradient below 45 nm might be due to abrupt changes in performance differences between models 3781 and 3783 for particles with CMD less than 45 nm. When considering that models 3783 and 3785 had comparable performances and model 3783 counted more particles than model 3781, the high COD gradient was likely a consequence of model 3781 under-counting particles smaller than CMD of 45 nm. This is further confirmed by the COD curve from models 3781 and 3785 where the COD also increased below the CMD of 45 nm. In this case, however, the rate of COD changes was lower than the rate of COD changes between models 3781 and 3783. This is presumably because model 3785, in general, counted fewer particles than model 3783. Therefore, the particles with CMD less than 45 nm disrupted model 3781 performance and consequently resulted in underestimation of particle number concentrations as shown in Fig. 3.

For intra-model comparisons, Fig. 9 presents COD changes across measured CMD ranges among the three units of TSI models 3781, 3783, and 3785. As discussed in Section 3.1, units 3781c,

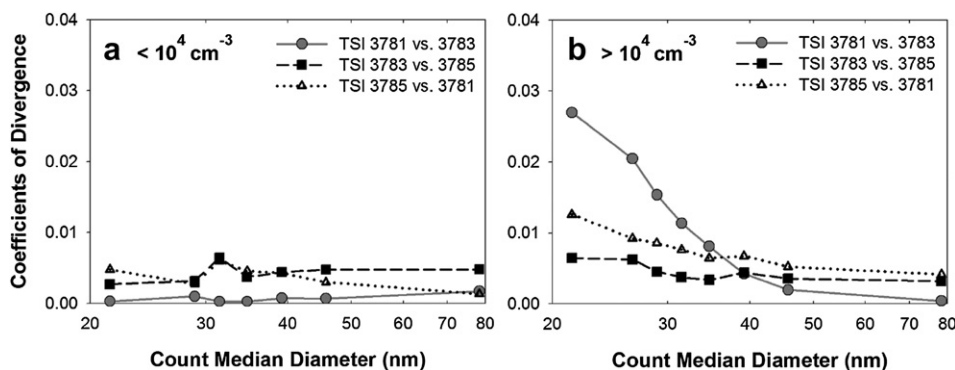


Fig. 8. Inter-model comparisons: the Coefficients of Divergence (CODs) among the three TSI WCPC models are plotted as a function of particle count median diameter (CMD) and particle number concentration ranges: (a) below  $10^4 \text{ cm}^{-3}$  (i.e.,  $10^3$ – $10^4 \text{ cm}^{-3}$ ) and (b) above  $10^4$  (i.e.,  $10^4$ – $3 \times 10^5 \text{ cm}^{-3}$ ).

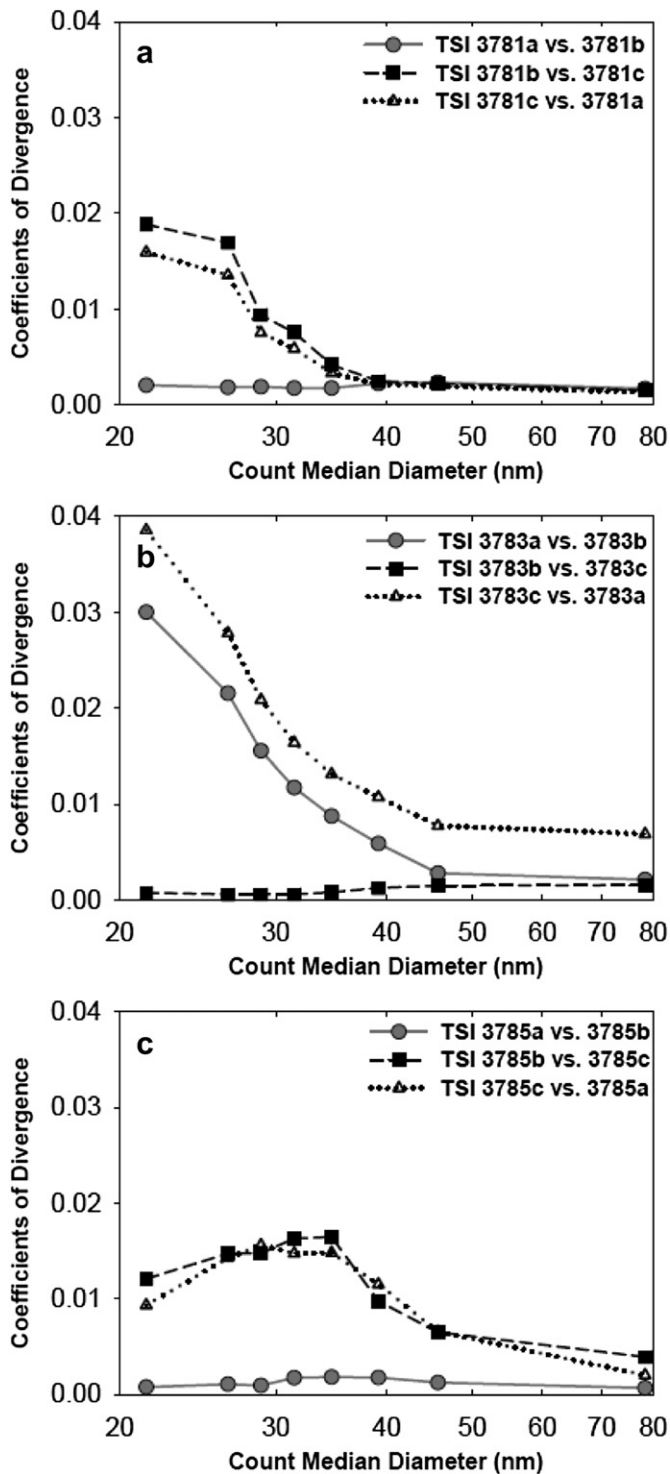


Fig. 9. Intra-model comparisons of the Coefficients of Divergence (CODs) for the three units of TSI WCPC models (a) 3781, (b) 3783, and (c) 3785 are plotted as a function of particle count median diameter (CMD).

3783a, and 3785c measured somewhat higher or lower values than the other two units. This observation is also explained by the data presented in Fig. 9. For example, Fig. 9-b shows that among the three 3783 units, the two high overall CODs were associated with 3783a. This was because concentration readings from instrument 3783a were higher than those from the other two units of the same model. However, the three COD curves are flat over CMD. This

pattern is similar to what has been observed in the COD curve for models 3783 and 3785 in Fig. 8. The flat COD curves suggested that CMD changes (i.e., particle size changes) had little impact on model 3783 readings. On the other hand, the cause of intra-model bias for 3781 and 3785 might be different from that of model 3783. Model 3781 presents significant COD increases in CMD less than 45 nm (Fig. 9-a) and model 3785 shows similar trend with less steep gradient of COD curves (Fig. 9-c). Since COD gradient between 3781a and 3781b seems flat and is similar for the case between 3785a and 3785b, the sudden changes in COD seem to be driven by 3781c and 3785c. These observations suggest that particle size may affect particle counting performances not only among different models but also among individual units of the same model. This particle size effect also seems to impact models 3781 and 3785 more dramatically than model 3783 throughout the measured particle size range. Considering that all three instrument units share the similar mechanical design, it is difficult to conclude one direct cause explaining why one instrument from each model behaved differently.

After excluding the data from what we believe to be poorly performed units from each model (i.e., 3781c, 3783a, and 3785c), we repeated the analysis as shown in Fig. 5-g,-h and -i. The magnitude of model differences was reduced by 25% for 3781 and 3783, 9% for 3783 and 3785, and 9% for 3785 and 3781. However, models 3781 and 3785 still measured particle concentrations 16% and 9% lower than model 3783, respectively. Therefore, the observed measurement differences might have been caused by inherent differences in model specific design and/or manufacturing processes which are beyond the scope of current work. For instance, although all three units of model 3783 were directly supplied from the manufacturer, the manufacturer later confirmed presence of problem with the electrical main board of 3783a.

### 3.3. Correction factors

The current findings lead to the development of post-data correction factors for the older WCPC models (i.e., models 3781 and 3785) to minimize inter-model bias. It should note that currently there is no reference standard instrument for particle number measurement. We chose to fit data to the model 3783 simply because it is the most recently developed TSI WCPC model and data from this study confirmed its superior stability across a wide particle concentration/size range.

In comparison with model 3783 data, the measurement bias of instrument models reached up to approximately 35% for model 3781 and 25% for model 3785 (Fig. 10). Because the theoretical maximum particle diffusion losses in the sampling lines remains less than 5%, the primary cause of model bias is thought to stem from the instrument itself. Therefore, the correction factors were derived from the 3-parameter exponential regression analyses shown in Fig. 10. The correction equations for WCPC models 3781 and 3785 as follows:

$$N_{\text{WCPC3783}} = 3.754 \times 10^5 \cdot e^{3.094 \times 10^{-6} \cdot N_{\text{WCPC3781}}} - 3.780 \times 10^5 \quad (2)$$

$$N_{\text{WCPC3783}} = 3.248 \times 10^5 \cdot e^{2.369 \times 10^{-6} \cdot N_{\text{WCPC3785}}} - 3.248 \times 10^5 \quad (3)$$

Eqs. (2) and (3) help minimize the intrinsic discrepancies from using recent WCPC models. The developed equations adjust the number concentration data ( $N_{\text{WCPC3781}}$  and  $N_{\text{WCPC3785}}$ ) collected from the older WCPC models 3781 and 3785 to fit the number concentration data from the most recently developed TSI model,

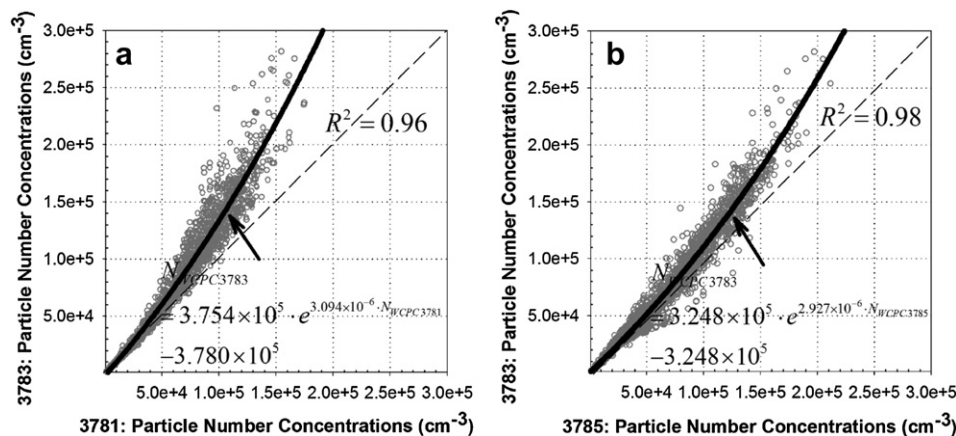


Fig. 10. Comparison between 15-min averaged data collected from TSI WCPC model (a) 3781 and (b) 3785 with model 3783. Solid lines represent 3-parameter exponential correction equations for each model comparison with TSI 3783.

3783 ( $N_{WCPC3783}$ ). The developed correction Eq. (3) results in good data fitting for the one month of data collected in this near-freeway environment. However, it is unknown how well the model would fit under different environments. It should also be noted that Eq. (2) is only applicable for particle number concentrations greater than  $1.5 \times 10^4 \text{ cm}^{-3}$ . When the particle number concentration is lower than  $1.5 \times 10^4 \text{ cm}^{-3}$ , the measurements of models 3781 and 3783 match well, and no post-data processing is needed. Eqs. (2) and (3) were derived on the basis that particle number concentration and size distribution are the primary factors affecting WCPC performance. The derived equations may be applicable to other near-freeway environment; however, different near-freeway ambient air might have different site-specific factors such as particle chemical compositions, which this study did not address.

#### 4. Conclusions

Measurements of UFPs were conducted for one month near a major freeway in order to compare the performance of different WCPC instrument units. An evaluation from nine WCPC units of three different models (i.e., TSI 3781, 3783, and 3785) found a certain level of bias between each model, while each unit of the same model resulted in less variability. Despite model differences, all WCPC units responded similarly in low concentration ranges ( $10^3$ – $10^4 \text{ cm}^{-3}$ ). However, in high concentration environments which usually occurred under downwind conditions, the variability and bias of each model measurement became larger, with the magnitude of the bias depended on the WCPC model. Specifically, TSI model 3781 consistently recorded the lowest concentrations among the three tested models mainly because of underestimating particles with CMD less than 45 nm. Model 3783 recorded the highest number concentrations, followed by model 3785 for ambient particle number concentrations greater than  $10^4 \text{ cm}^{-3}$ . The discrepancies between the model 3783 and 3785 measurements were minimal up to a number concentration of  $10^5 \text{ cm}^{-3}$ , but found higher bias in number concentration above  $10^5 \text{ cm}^{-3}$ . In an effort to increase the linear relationship, we investigated the effect of using longer averaging time intervals and found that an acceptable data correlation could be achieved using an averaging time of 15 min and above. Based on these one-month data, TSI model 3783, designed for long-term monitoring, provides relatively consistent data with the least sensitivity to particle size among the evaluated models. A long term evaluation of the reliability of TSI 3783 is currently underway and will be discussed in a subsequent paper. To minimize instrumental or

model differences, post-data correction equations were proposed to adjust the data from TSI models 3781 and 3785 to model 3783 using 3-parameter exponential models.

#### Acknowledgments

This study complements work in progress partially supported by the National Science Foundation's CAREER Award under contract # 32525-A6010 AI, and resources from the South Coast Air Quality Management District (AQMD) and the California Air Resources Board (ARB). The authors thank TSI Inc. for providing several WCPC units. The authors also thank AQMD and ARB staff for their assistance with the field measurements. Any opinions, findings, conclusions or recommendations expressed in this report are those of the authors and do not necessarily reflect the views of the National Science Foundation, the AQMD, or the ARB.

#### References

- Aitken, J., 1890. On a simple pocket dust-counter. *Proceedings of the Royal Society of Edinburgh* 18, 39–53.
- CalTrans, 2010. Performance Measurement System (PeMS). California Department of Transportation (CalTrans), Sacramento, CA.
- Donaldson, K., Brown, D., Clouter, A., Duffin, R., MacNee, W., Renwick, L., Tran, L., Stone, V., 2002. The pulmonary toxicology of ultrafine particles. *Journal of Aerosol Medicine-deposition Clearance and Effects in the Lung* 15, 213–220.
- Gilmour, P.S., Ziesenis, A., Morrison, E.R., Vickers, M.A., Drost, E.M., Ford, I., Karg, E., Mossa, C., Schroepel, A., Ferron, G.A., Heyder, J., Greaves, M., MacNee, W., Donaldson, K., 2004. Pulmonary and systemic effects of short-term inhalation exposure to ultrafine carbon black particles. *Toxicology and Applied Pharmacology* 195, 35–44.
- Hering, S.V., Stolzenburg, M.R., 2005. A method for particle size amplification by water condensation in a laminar, thermally diffusive flow. *Aerosol Science and Technology* 39, 428–436.
- Hering, S.V., Stolzenburg, M.R., Quant, F.R., Oberreit, D.R., Keady, P.B., 2005. A laminar-flow, water-based condensation particle counter (WCPC). *Aerosol Science and Technology* 39, 659–672.
- Hinds, W.C., 1999. *Aerosol Technology: Properties, Behavior, and Measurement of Airborne Particles*, second ed. Wiley, New York.
- Iida, K., Stolzenburg, M.R., McMurry, P.H., 2009. Effect of working fluid on sub-2 nm particle detection with a laminar flow ultrafine condensation particle counter. *Aerosol Science and Technology* 43, 81–96.
- Jaques, P.A., Kim, C.S., 2000. Measurement of total lung deposition of inhaled ultrafine particles in healthy men and women. *Inhalation Toxicology* 12, 715–731.
- Kreyling, W.G., Semmler, M., Erbe, F., Mayer, P., Takenaka, S., Schulz, H., Oberdorster, G., Ziesenis, A., 2002. Translocation of ultrafine insoluble iridium particles from lung epithelium to extrapulmonary organs is size dependent but very low. *Journal of Toxicology and Environmental Health – Part A* 65, 1513–1530.
- Kulmala, M., Mordas, G., Petaja, T., Groenholm, T., Aalto, P.P., Vehkamaeki, K., Hienola, A.I., Herrmann, E., Sipilae, M., Riipinen, I., Manninen, H.E., Haemeri, K., Stratmann, F., Bilde, M., Winkler, P.M., Birmili, W., Wagner, P.E., 2007. The

- condensation particle counter battery (CPCB): a new tool to investigate the activation properties of nanoparticles. *Journal of Aerosol Science* 38, 289–304.
- McMurry, P.H., 2000. A review of atmospheric aerosol measurements. *Atmospheric Environment* 34, 1959–1999.
- Oberdorster, G., Sharp, Z., Atudorei, V., Elder, A., Gelein, R., Lunts, A., Kreyling, W., Cox, C., 2002. Extrapulmonary translocation of ultrafine carbon particles following whole-body inhalation exposure of rats. *Journal of Toxicology and Environmental Health – Part A* 65, 1531–1543.
- Petaja, T., Mordas, G., Manninen, H., Aalto, P.P., Hameri, K., Kulmala, M., 2006. Detection efficiency of a water-based TSI condensation particle counter 3785. *Aerosol Science and Technology* 40, 1090–1097.
- Stolzenburg, M.R., McMurry, P.H., 1991. An ultrafine aerosol condensation nucleus counter. *Aerosol Science and Technology* 14, 48–65.
- TSI, 2003. Model 3785 Water-based Condensation Particle Counter: Operation and Service Manual. TSI Inc., Shoreview MN, USA.
- TSI, 2005. Model 3781 Water-based Condensation Particle Counter: Operation and Service Manual. Shoreview MN, USA.
- TSI, 2011. Model 3783 Water-based Condensation Particle Counter: Operation and Service Manual. TSI Inc., Shoreview MN, USA.
- Zhu, Y.F., Hinds, W.C., Kim, S., Shen, S., Sioutas, C., 2002. Study of ultrafine particles near a major highway with heavy-duty diesel traffic. *Atmospheric Environment* 36, 4323–4335.